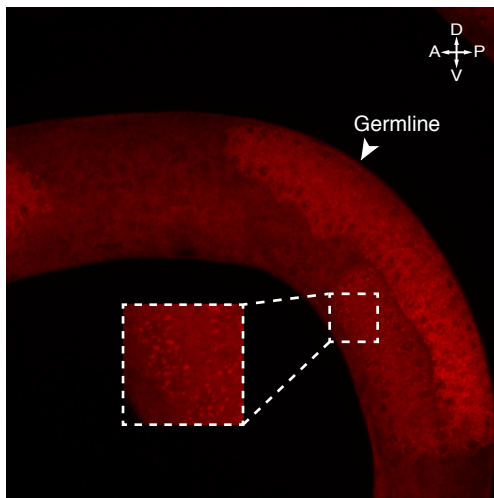
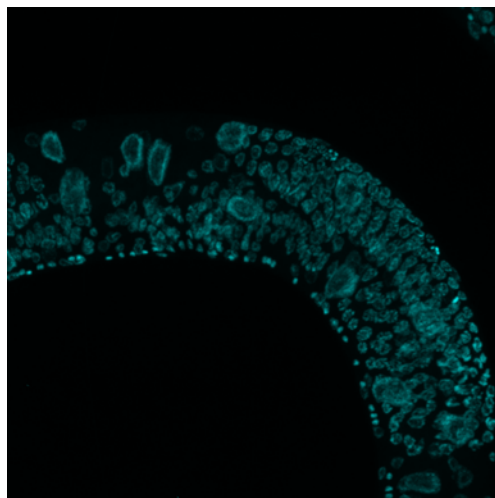


car-1 smFISH



DAPI



merge

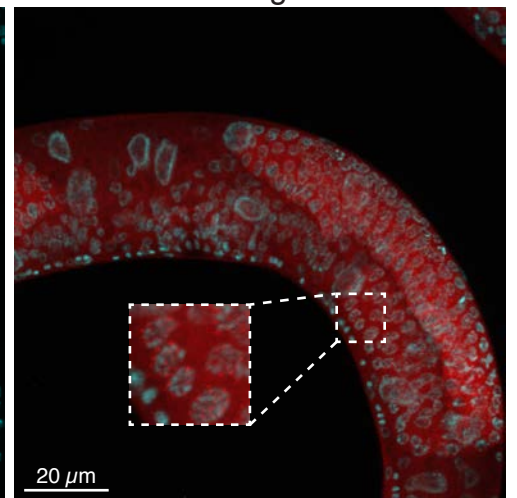


Figure S1. *car-1* mRNAs are present in the *C. elegans* germline. Related to Figure 1.

smFISH of *car-1* mRNAs showing cytoplasmic puncta in the germline. DAPI counterstain for DNA. Scale bar, 20 μ m.

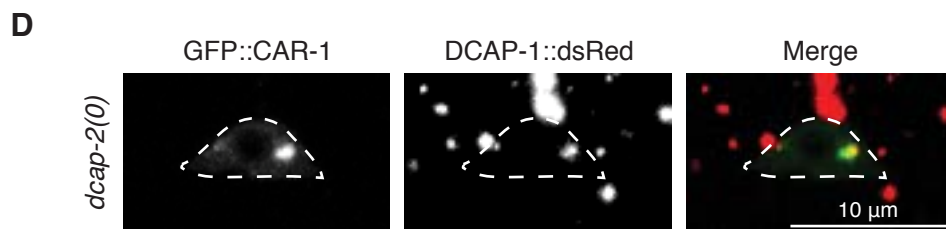
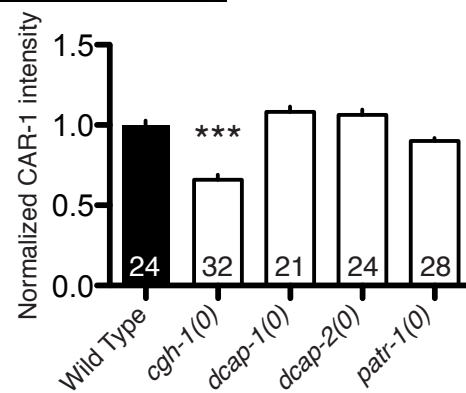
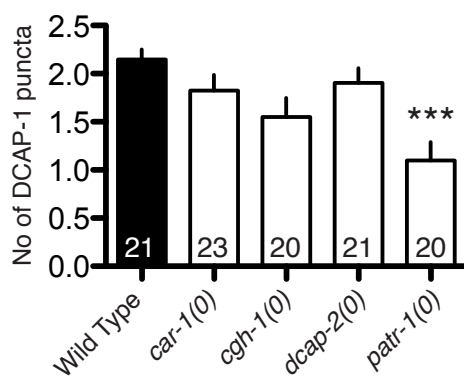
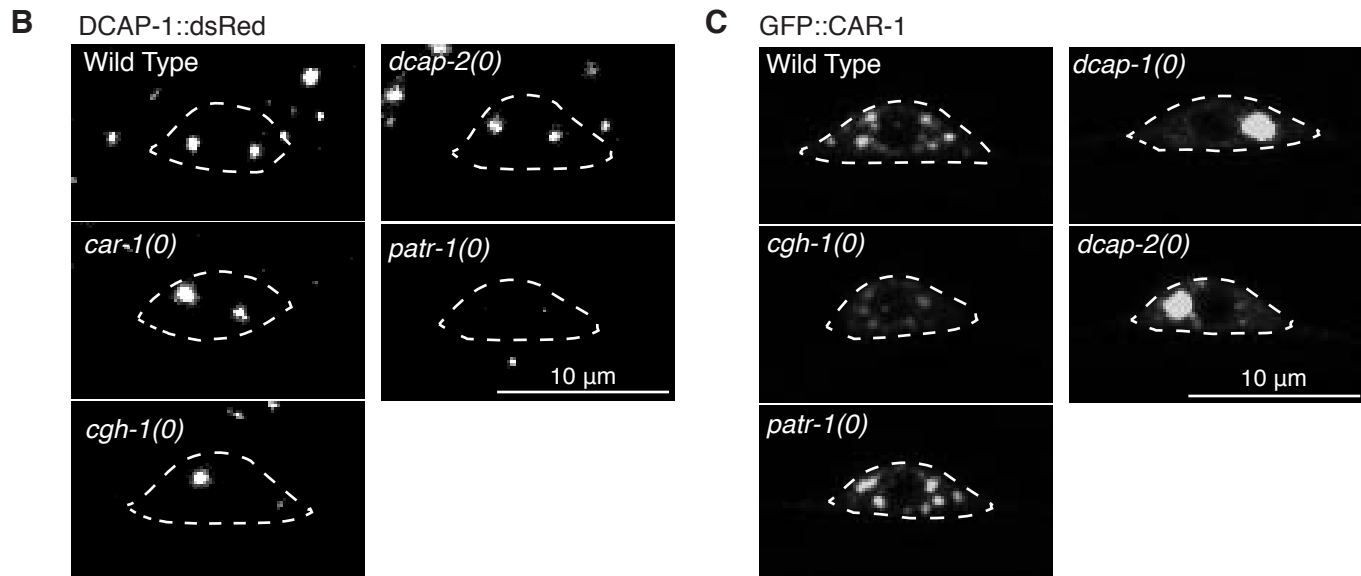
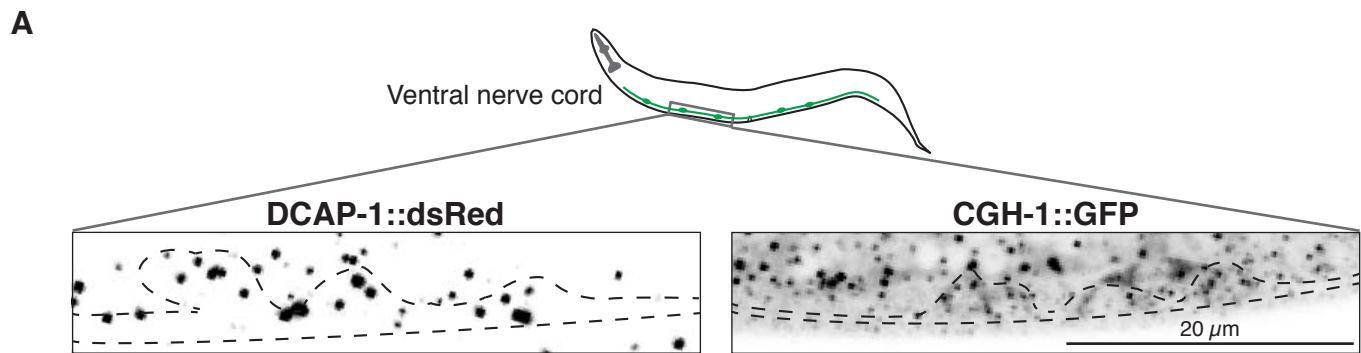


Figure S2. Localization of DCAP-1 and CAR-1 in mRNA decay mutants. Related to Figure 1.

- A) Localization of DCAP-1 [*Pdcap-1*-DCAP-1::*dsRed(bpIs37)*] or CGH-1 [*Pcgh-1*-CGH-1::*GFP(dhIs1000)*] within the ventral nerve cord of cholinergic motor neurons (outlined). The cholinergic motor neurons are labeled with *Punc-17*-*GFP(vsls48)* or *Punc-17*-mCherry(*nuls321*). DCAP-1 and CGH-1 showed similar localization in GABAergic motor neurons (not shown). The ventral nerve cord is outlined. Scale bar, 20 μ m.
- B) Top shows confocal images of DCAP-1::*dsRed(bpIs37)* localization in indicated mRNA decay mutants. Bottom shows quantitation of DCAP-1 puncta in the PLM cell body. Sample size is indicated in the bar.
- C) Top shows confocal images of GFP::*CAR-1 (juSi338)* localization in indicated mRNA decay mutants. Bottom shows quantitation of DCAP-1 puncta in the PLM cell body. Statistics: one-way ANOVA with Bonferroni's post test; *** $p < 0.001$.
- D) The loss of *dcap-2* results in accumulation of CAR-1 into enlarged puncta, which colocalizes with the DCAP-1 granules. Scale bar, 10 μ m.

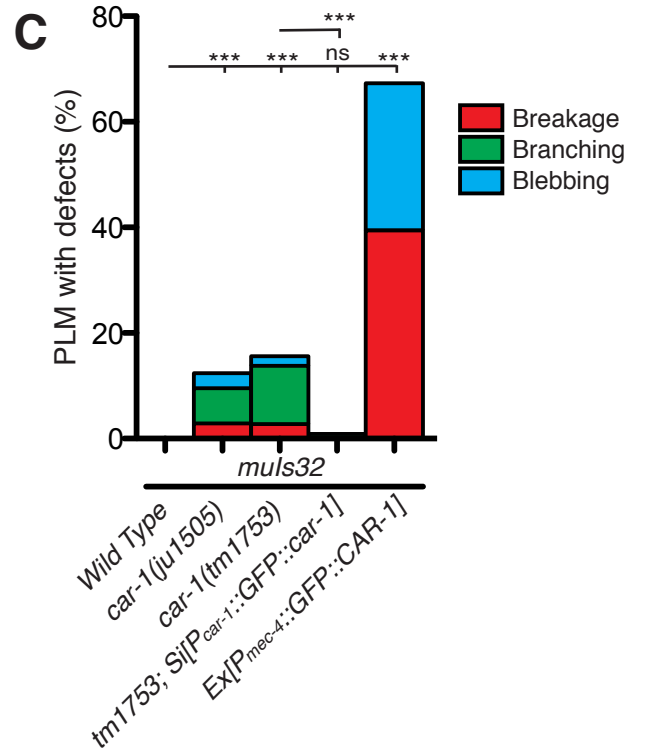
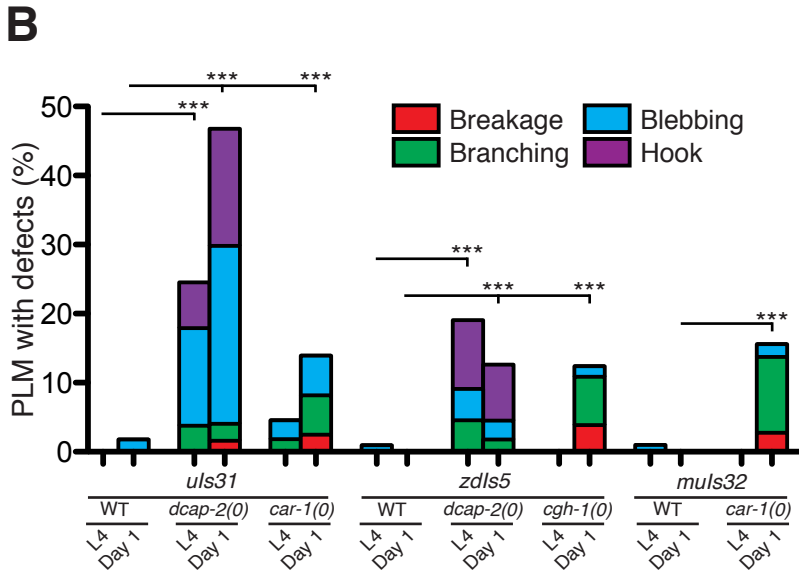
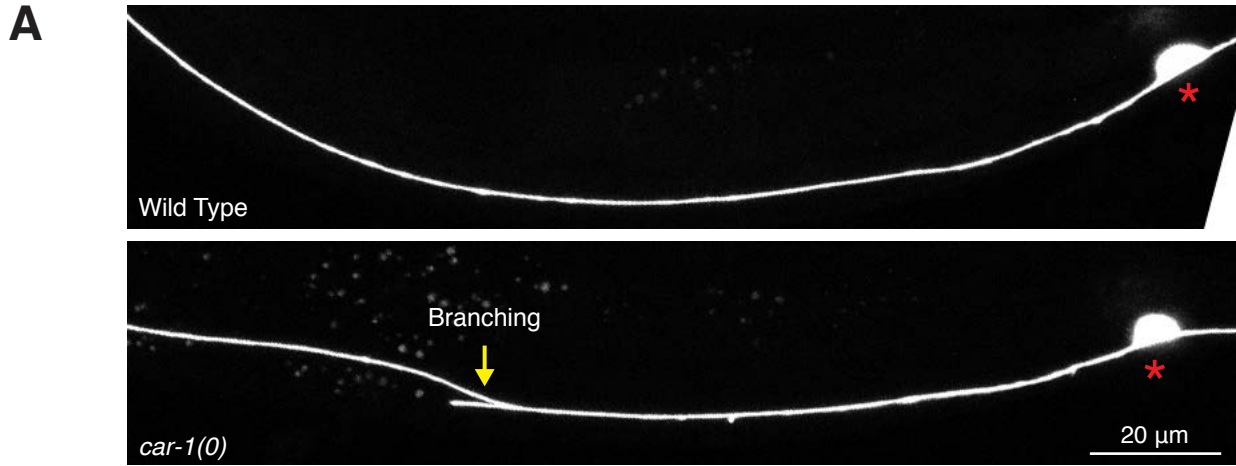


Figure S3. Re-expression of *car-1* rescues axonal morphology in *car-1(0)* mutants.

Related to Figure 2.

- A) Posterior end of the PLM axons in wild type or *car-1(0)* mutants showing branching phenotype. Red * marks position of the cell body, yellow arrowhead marks the position of branched axons. Anterior to the left.
- B) Quantification of abnormal PLM phenotypes in wild type and mRNA decay mutants. TRNs were labeled with *Pmec-17-GFP(uls31)*, *Pmec-4-GFP(zdls5)* or *Pmec-7-GFP(muls32)*. N≥100. Statistics: Fisher's exact test; ** p<0.01, *** p<0.001; ns, not significant (P>0.05).
- C) Abnormal PLM morphology of *car-1(0)* mutant was observed using two independent alleles, in two independent transgenic backgrounds (*uls31* and *muls32*). *Pcar-1-GFP::CAR-1(juSi343)* rescued the PLM defects in *car-1(0)* whereas over-expression of CAR-1 (Ex[*Pmec-4::GFP::CAR-1*]) resulted in serious PLM defects. Day 1 adults were observed and quantified. N≥100. Statistics: Fisher's exact test; ***p<0.001; ns, not significant (P>0.05).

A

Ce_MICU-1	MLHCSFLRVIPIKNASKRLIIIVRSLTSAPAKTSEAEKQDQSLKNIDAGEKYTALGNIRQKKDVHYHTDRASGVGVSHYSSSVYQHRPFIWPLRKLKLY-----HWNYALVIAGMV-	109
Human_MICU1	-----MFRNLSLSALAEALVAGSRWYHGGSQPIQIR-----RRLLM-----MVAFLGASAV-	44
Ce_C56A3.6	-----MNRVLSRFWGFSTKHRQHIL	20
Human_MICU2	-----MAAAAGSC-----ARVAAWGKLRRLGLAVS	25
Human_MICU3	-----MAALRRLWPPRVPSPPLCAHQPLLGPWGRPAVTTLGLP	39
Ce_MICU-1	-----ILMSDFEWLKDQIK-----SASLP--FRPE----ASQKE--EV-T--ESNGEVEVKEKPKKKKLGFRERRI IEYE-DRLRLYSTPDKIFRYFATL	188
Human_MICU1	-----TASTGLLWKRAHAE-----SPPCVDNLKSDIGDKGNKDEGDV-CNHEKKTADLAPHPEEKKKRSRGRDRKVMYEY-NRIRAYSTPDKIFRYFATL	134
Ce_C56A3.6	NQRIVERTS-----ARNAVLT-AAAGIGTSIGAYQLIDTARAGILDGS-----DDASRHNVTTDHKLTKRELRFQFASV	89
Human_MICU2	RQAVR-----SPGPL-----AAVAGALAGAGAAWHHS-----RVSVAAADGSGFTVSAQKNVEHGI IYIGKPSLRKQRFMQFSSL	96
Human_MICU3	GRPFSSREDEERAVAEAAWRRRRRWGELSVAAAAGGLVGLVYQLYGDPAGSPATGRPSKSAATEPEDPPRGRGMLPIPVAAKETVAI-GRTDIEDLDLY---ATSRERRRRLFASII	155
Ce_MICU-1	KIIDPNEDSGRFEVFMTPEDFLRSFTPGVMQPRRWGLDSFKNYN----PEKHKRHKFSDDPS IFYKLGENGLINFSDYFLFMTLLSTSHADFALAFKIFDVGNGALDKEEFTKQVQQLIM	304
Human_MICU1	KVIS---EPGEAEVFMTPEDFVRSITPNEKQPEHLGDQYIIKRFDGKKISQEREKFADEGS IFYTLGECGLISFSDYIFLTTVLS TPQRNFE IAFKMFDLNGDGEVDMEEFEVQVQSIIR	251
Ce_C56A3.6	E-----YDDVIYMSPMDFIDSLTLDAPRERVYRR-VLKEKDI-QRILKKTTPFRSGGKHFFRTMDQSGI ISYSEYIFLLTLLTKSKAAPRIAF LMFDEDDNGNIDRDEFMLIRSLTS	199
Human_MICU2	E-----HEGEYMTPRDFLFVSMFQEMERKTSVK-KLTKKDI-EDTLGGIQTAA-CGSGTFRDLGDKGLISYTYEYLFLLTILTKPHSGFHFVAFKMLD TDGNEMIEKREFFKQKIIIS	205
Human_MICU3	E-----CEGQLFMTYPDYILAVTTDEPKVAKTWK-SLSKQEL-NQMLAETPPVWKGSKLFRNLKEKGVISYTYEYLFLLCILT KPHAGFR IAFNMFD TDGNEMVDDKKEFLVLQEIIFR	265
Ce_MICU-1	SQTTVGQRHRDHITP-----N-----QSFVETNSALETYFFGKDGKGSLSSEKFI EFQERLQHDILK	362
Human_MICU1	SQTSMGMRHRDRPTT-----G-----NLTSGKLSALTYFFGADLKGKLTIKNFLEFQRKQHDVLK	309
Ce_C56A3.6	SLRSTTRVQPSTASDEEDRRESCQLDAADYHFVAFSRI---GADRLFTGADSYAVMFTIARMFASKAATLSGTRLVHKSEEEVVRKQDTLLLLHLFGRGNATLSFDEFQOQYENLQEEELME	316
Human_MICU2	KQDDLMTVK-----TNET-----GYQE-----AIVKEPEINTTLMRFFGKRGQRKLHYKEFRFRFMENLQTEIQE	265
Human_MICU3	KKNEKREIK-----GDEEKRAMRLQLYGYHSPNSVLKTDABEELVS---RSYW---DTLRR---NTSQALFSDLAERADDITSLVTD TLLVHFPGKKAELNFPDFYRMDNLQTEVLE	373
Ce_MICU-1	MEFERRDALDNPGLINEDSFAQLLLLHAQINEKQKHM LKRVKRRFKGENLKGISFGETKAPFFELYHIDDVDIALHFHKMAGMS IDAKLLQRVAVKVTGIP LSDHVVDVVITLFDNDL	482
Human_MICU1	LEFERHDPV---DGRITERQFGGMLLAYSGVQSKL TAMQRQLKHKHFK--GKGLTFQEVENFFFLKNINDVD TALSFYHMAGASLDKVTM QQVARTVARVELSDHVCVVFALFDCDG	424
Ce_C56A3.6	IEFYEFPA---RGKTAISPVD FARILLRYSIVNFDDYHKYLQRVQE--KSDDEE PGISLSQWATFSRFLNNALEFQSAVRLYVNSNVPVSEPEFARAVGCTIGKELDPVVVSMIFRIFDENN	432
Human_MICU2	MEFLQFS---KGLSFMRKEDFAEWLLFFNTNEN--KDIYWKNVRE--KLSAGESISLDEFKSFCHFTTHLEDFALAMQMFSLAHRPVRLAEFKRAVKVATGQELSNLLD TVKIFDLDG	378
Human_MICU3	IEFLSYS---NGMNTISEEDFAHILLRYTNVEN--TSVLENVRY--SIPEEKGITDFEFSFFQFLNNLEDFALALNMYNFASRS IQDEFKRAVYVATGLKFSPHLVNTVFKIFDVDK	486
Ce_MICU-1	DGKLSHEEMVAVMRRRRRGLERPRDTGLFRLFDVAVLECGKRAYHASPLPFY-----	534
Human_MICU1	NGELSNKEFVSIKQRLRMGLEPKDMGFTRLMQAMWKAQETAWDFALPKQ-----	476
Ce_C56A3.6	DGTLSYPEPLAVMSDRDLHRGLRGRLEKP---WGKPFKNCVISEVSR-----	477
Human_MICU2	DECLSHEEPLGLVKNRMRGLWVPOH---QSIQEYWKCVKESIKRGVKEVWQAGKGLF	434
Human_MICU3	DDQLSYKEFIGIMKDRDLHRGFRGYKT-V---QKYPTFKSCLKKELHSR-----	530



B MICU-1::GFP(*ju1783*)

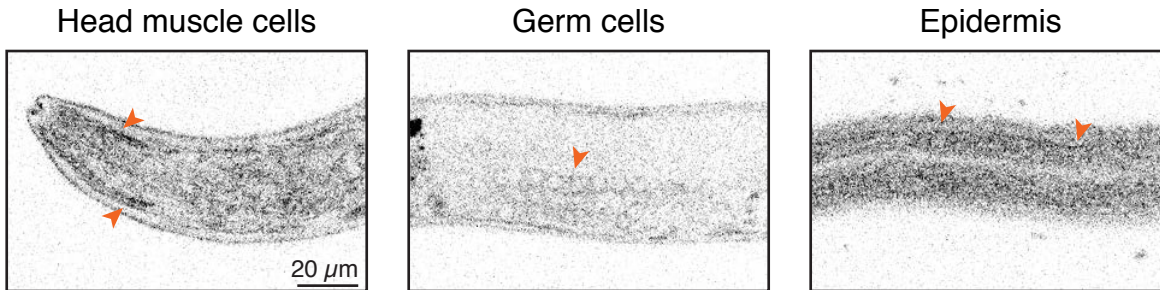


Figure S4. *C. elegans* MICU proteins are related to mammalian MICU. Related to Figure 6.

- A) Multiple protein sequence alignment and phylogenetic tree for MICU1 family proteins. Accession numbers: *C. elegans* MICU-1 isoform D (Q95PZ2), Human MICU1 (Q9BPX6), *C. elegans* C56A3.6 (Q18874), human MICU2 (Q8IYU8), human MICU3 (Q86XE3). Sequence alignment and phylogenetic tree were generated using ClustalOmega (<http://www.ebi.ac.uk/Tools/msa/clustalo/>) with default settings. Among human MICU family members, MICU1 is closest to *C. elegans* MICU-1; MICU2 and MICU3 are equally related to C56A3.6.
- B) Representative confocal images of endogenous MICU-1::GFP(*ju1783*) in head muscles, germ cells and the epidermis.

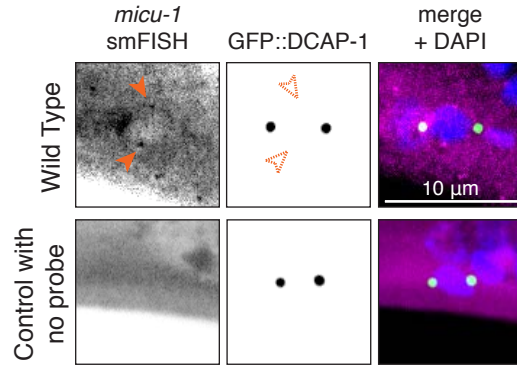
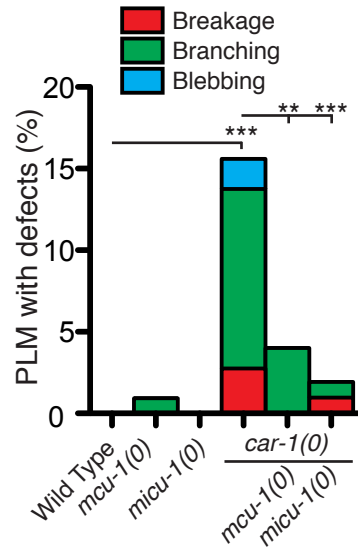
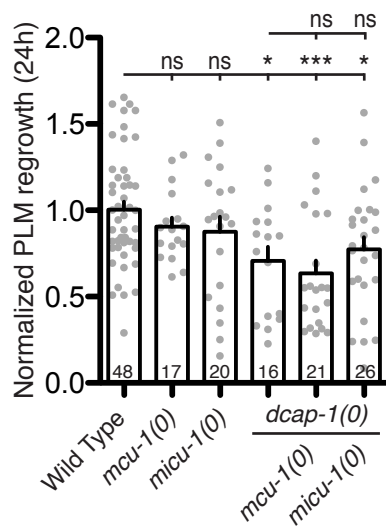
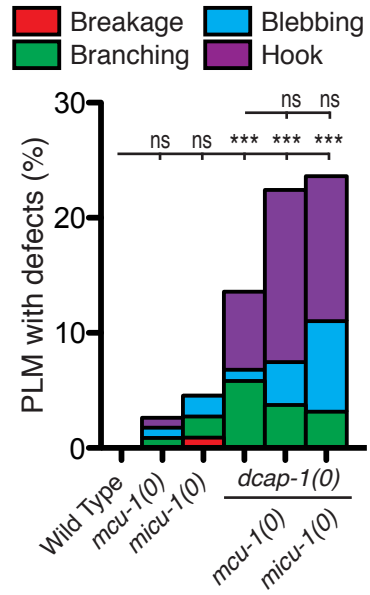
A**B****C****D**

Figure S5. Loss of *mcu-1* or *micu-1* does not suppress *dcap-1(0)* phenotypes.

Related to Figure 6 and 7.

- A) smFISH of *micu-1* mRNA. *micu-1* mRNAs do not colocalize with GFP::DCAP-1 expressed in TRNs [*Pmec-4-GFP::DCAP-1(juEx8024)*].
- B) Abnormal PLM morphology of *car-1(0)* mutant is rescued by deletion of *mcu-1* or *micu-1*. N≥100. Statistics: Fisher's exact test; **p<0.01; ***p<0.001.
- C) Reduced axon regrowth in *dcap-1(0)* mutant is not rescued by deletion of *mcu-1* or *micu-1*. Statistics: one-way ANOVA with Bonferroni's posttest; *p<0.05; ***p<0.001; ns, not significant. Sample size is indicated in the bar.
- D) Abnormal PLM morphology of *dcap-1(0)* mutant is not rescued by deletion of *mcu-1* or *micu-1*. N≥100. Statistics: Fisher's exact test; ***p<0.001; ns, not significant.

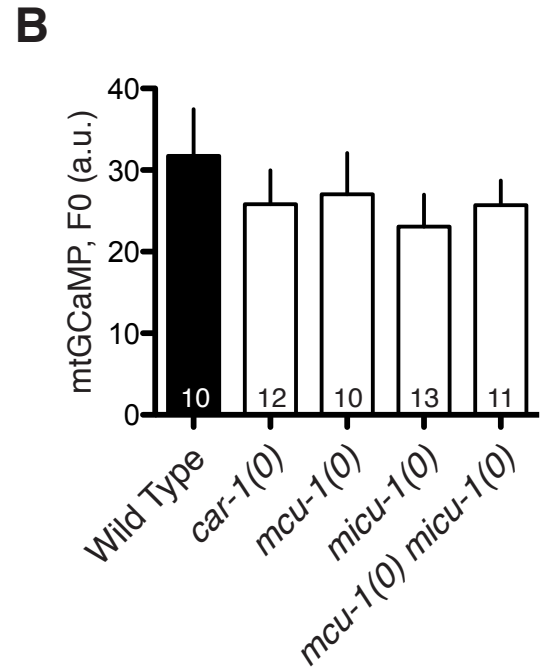
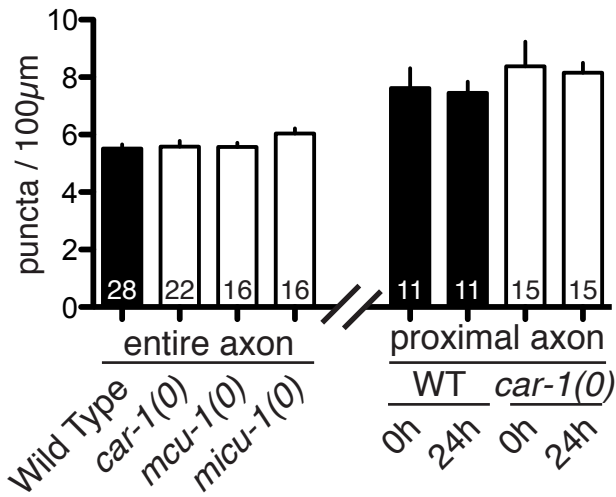
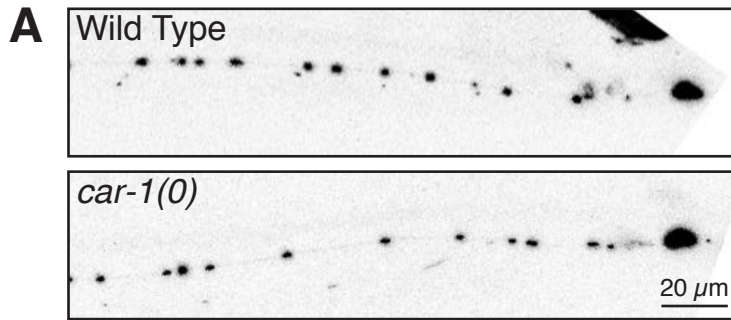


Figure S6. *car-1*, *mcu-1*, and *micu-1* mutants display normal axonal mitochondrial distribution and baseline $[Ca^{2+}]_{mt}$. Related to Figure 7.

- A) Mitochondria density in PLM neurons was not affected in *car-1(0)*, *mcu-1(0)* and *micu-1(0)* mutants. Top shows representative images of mitochondria localization [P*mec-7*-tagRFP::mito(*jsIs1073*)] in PLM neurons in wild type and *car-1(0)*. Bottom shows quantification of mitochondria puncta in PLM neurons in the entire uninjured axon (left), or proximal axon (right) at 0 h or 24 h post-axotomy. Sample size is indicated in the bar.
- B) Baseline levels of mito-GCaMP (F0) in different mutants before axotomy. Sample size is indicated in the bar.

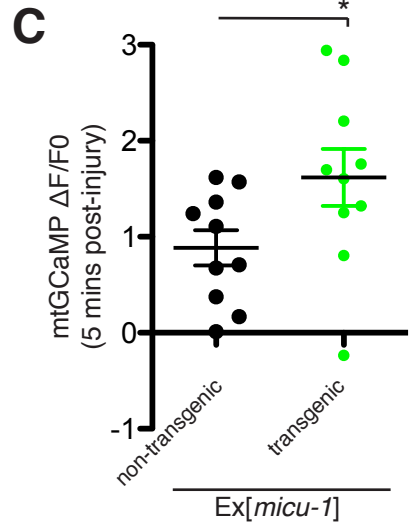
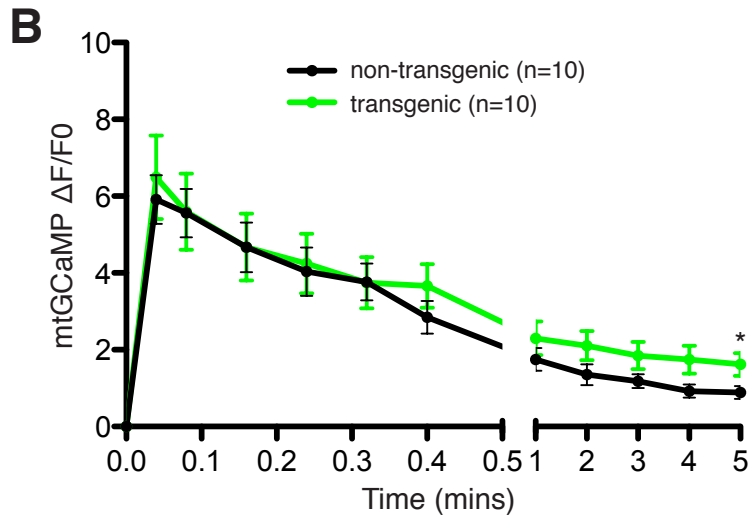
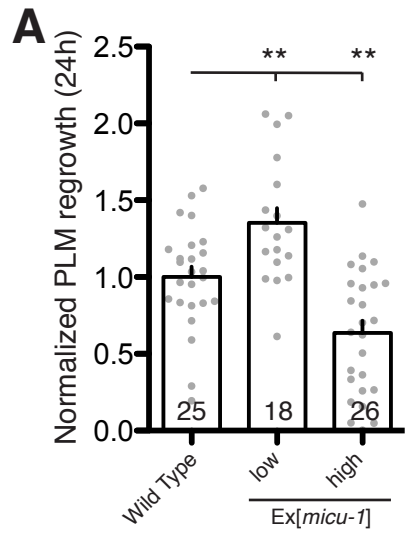


Figure S7. Overexpression of *micu-1* phenocopies *car-1(0)* mutants in axon regrowth. Related to Figure 7.

A) Slight overexpression of *micu-1* (2ng/ μ l, *juEx8048*) results in increased PLM axon regrowth, whereas high overexpression of *micu-1* (10ng/ μ l, *juEx8050*) results in decreased PLM axon regrowth. Bars indicate mean \pm SEM. Statistics: one-way ANOVA with Bonferroni's post test; ** $p < 0.01$.

B) mtGCaMP fluorescence intensity ($\Delta F/F_0$) over 5 minutes post-axotomy. Transgenic animals (*juEx8048*) show sustained $[Ca^{2+}]_{mt}$ uptake upon axon injury. Non-transgenic animals are siblings from the same strain. Statistics: Unpaired t-test against non-transgenic animals; * $p < 0.05$.

C) mtGCaMP fluorescence intensity ($\Delta F/F_0$) at 5 minutes post-axotomy in genotypes indicated. Each dot represents a mtGCaMP in an animal. Statistics: Unpaired t-test; * $p < 0.05$.

Gene name	Allele number	Breakpoints/Mutations
<i>car-1</i>	<i>ju1505</i>	AGTTTGAGCTTACCT...(698bp deletion+9bp insertion)...GTCGTGATGATGTC
<i>car-1</i>	<i>ju1506</i>	TTTTCGTTATTTTTT... (1110bp deletion) ...CCGTTAGGCCAAATC
<i>micu-1</i>	<i>ju1155</i>	CGTTGATAAATCGACCGCGT...(1001bp deletion+218bp insertion)...ACAGTGGACGCTTTGAAGTT
<i>micu-1</i>	<i>ju1156</i>	CGCTCCGTTGATAAATCGAC...(1014bp deletion)...CGCTTTGAAGTTTTTCATGAC

Table S2. Description of new alleles created in this study. Related to Figure 3 and 7.